Direct Evidence for Surface Plasmon-Mediated Enhanced Light Transmission through Metallic Nanohole Arrays

Hanwei Gao, Joel Henzie, and Teri W. Odom*

Department of Chemistry, Northwestern University, 2145 Sheridan Road, Evanston, Illinois 60208

Received July 19, 2006

ABSTRACT

This paper provides direct evidence for the role of surface plasmons in the enhanced optical transmission of light through metallic nanoscale hole arrays. Near-field optical images directly confirmed the presence of surface plasmons on gold nanohole arrays with interhole spacings larger than the surface plasmon wavelength. A simple interference model provides an intuitive explanation of the two types of fringe wavelengths observed in the near-field optical images. Far-field spectroscopy revealed a surface plasmon band that contributed a factor >8 to the transmission enhancement. Furthermore, silicon nanohole arrays did not exhibit any features in the near-field, which demonstrates that metallic materials are necessary for enhanced light transmission through nanohole arrays.

Ground-breaking discoveries in diverse fields such as photonics,[1−5] chemistry,[6,7] and biophysics[8,9] have relied on surface plasmon polaritons (SPPs) to confine and enhance light in the optical near-field. Interest in the fundamental science of SPPs was revived in part by the report of extraordinary light transmission through metallic subwavelength hole arrays[1] which did not follow classical optical theory.[10] SPPs were initially proposed to assist in this enhanced transmission,[11] although subsequent theoretical and experimental work has claimed different mechanisms.[12−14] Understanding the role of SPPs in enhanced transmission is crucial for exploiting its nature to beat diffraction in applications such as subwavelength optics and nanophotonics. Here we present direct evidence for SPP-mediated enhanced transmission through gold nanohole arrays by combining, for the first time, near-field and far-field measurements of films with interhole spacings larger than the SPP wavelength. We propose a simple model that explains two types of interference in the near-field patterns and measure an SPP-enhancement factor > 8 in our gold hole arrays.

Surface plasmon polaritons are collective charge oscillations that are produced by the resonant interaction between light and free electrons at the interface of metallic and dielectric materials. Additional momentum is required to couple light into SPPs because of their different dispersion relations.[15] This condition is typically satisfied by a cor-

rugated surface such as a grating or by evanescent coupling with a prism or a near-field probe.[15,16] Far-field spectroscopy has been the main approach for investigating enhanced transmission through subwavelength hole arrays;[17,18] however, far-field measurements cannot unambiguously identify the presence of SPPs since their electromagnetic field is trapped in the near-field region of the metal−dielectric interface. Near-field scanning optical microscopy (NSOM) is one technique that can directly image SPPs on a metal surface. In this Letter, we have combined NSOM imaging and far-field spectroscopy on isolated nanoholes and nanohole arrays in gold films to address the question of SPP-enhanced optical transmission.

Free-standing films of gold perforated with nanoscale holes were fabricated by a technique we recently developed called PEEL,[16,19] which is a combination of **P**hase-shifting photolithography, **E**tching, **E**lectron-beam deposition, and **L**iftoff. This versatile procedure can generate arrays of holes with arbitrary spacings (a_0) and film thicknesses (t) controlled to 1 nm. Because the propagation length of SPPs (δ_{SP}) on a flat gold surface is less than 10 μm under excitation of 633-nm light,[20] nanoholes separated by distances larger than δ_{SP}, such as $a_0 = 25$ μm in Figure 1a, can be considered as isolated holes. Near-field optical images of isolated holes (diameter $d = 250$ nm) in gold films of two different thicknesses ($t = 50$ and 180 nm) were acquired in collection mode through an Al-coated pulled optical fiber probe (Figure 1b,c). The excitation source was a linearly polarized 633-
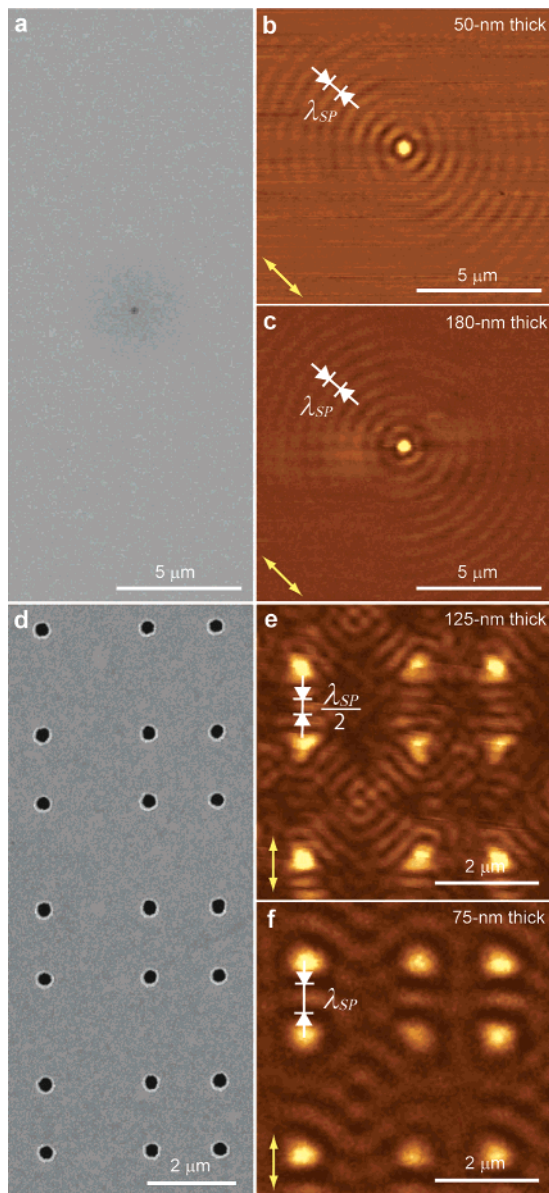
Figure 1. SEM and NSOM images of nanohole arrays in gold films. (a) Single 250-nm hole in a 25-μm spaced array. (b and c) Near-field images of isolated holes in gold films (a) that are 50 nm and 180 nm thick. White arrows denote the wavelength of the fringes, which is identical to the surface plasmon wavelength (λ_{SP}). Yellow arrows indicate the polarization direction of incident light. (d) Array of 250-nm holes with interhole spacing $a_0 \sim 2$ μm. (e) Near-field image of hole arrays in a 125 nm thick gold film. White arrows denote the wavelength of the fringes, which is equal to half of the surface plasmon wavelength ($\lambda_{SP}/2$). (f) Near-field image of hole arrays in a 75 nm thick gold film. White arrows denote the wavelength of the fringes, which is equal to the surface plasmon wavelength (λ_{SP}). Yellow arrows indicate the polarization direction of incident light.

nm He−Ne laser. Both films exhibited fringes surrounding the holes. The measured fringe-wavelength (λ_f) was 603 nm, which is identical to the SPP-wavelength (λ_{SP}) at the gold−air interface (Supporting Information), and the fringe direction was along the polarization of the incident light. An isolated hole at the top surface of a film (i.e., the surface closest to the NSOM probe) can act as a source of SPPs,[21] and hence the observed fringes can be attributed to interfer-
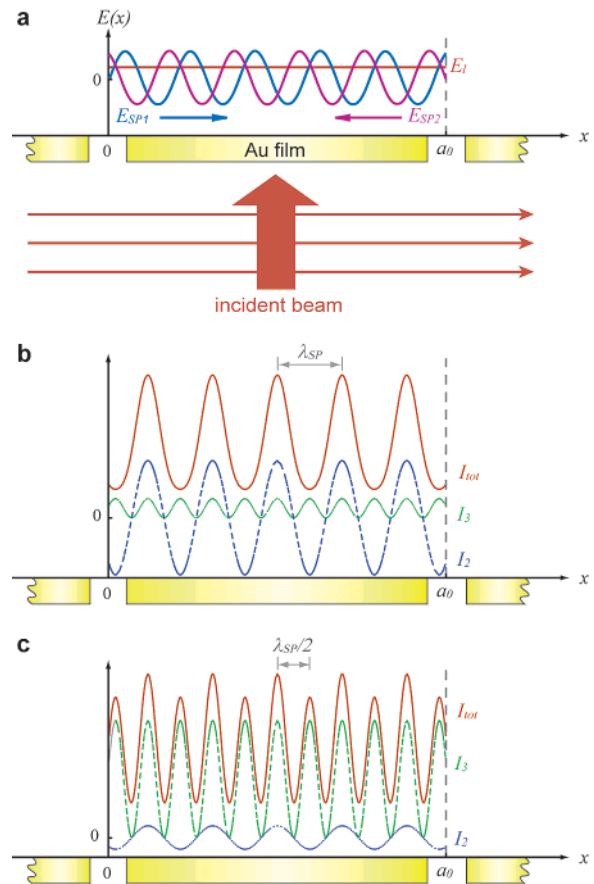
Figure 2. Scheme of the 1D interference model. (a) In-plane electric field of SPPs between adjacent holes and directly transmitted light under incident light polarized along the x-direction. (b) Total intensity is dominated by I_2 if the A_l/A_{SP} ratio is large, and $\lambda_f = \lambda_{SP}$. (c) Total intensity is dominated by I_3 if the A_l/A_{SP} ratio is small and $\lambda_f = \lambda_{SP}/2$. The fringe-wavelength λ_f is primarily determined by the A_l/A_{SP} ratio.

ence between the SPPs launched by the hole and the light transmitted directly through the film.[22]

To resolve the near-field optical distribution between holes in an array, we fabricated nanohole arrays with a_0 less than δ_{SP} but still greater than λ_{SP} (Figure 1d). We initially focused on films with thicknesses between those of the isolated holes in parts b and c of Figure 1. Surprisingly, for 250-nm hole arrays with $a_0 \sim 2$ μm, λ_f on a 125 nm thick gold film changed to $\lambda_{SP}/2$ even though λ_f remained constant at λ_{SP} for a 75-nm film (parts e and f of Figure 1). To obtain a physical understanding of this unexpected dependence of λ_f on film thickness, we developed a simple model based on the interference between SPPs launched by the holes and light transmitted through the film. Since $a_0 \sim 2$ μm is much shorter than δ_{SP}, the interaction between the holes is essential for interpreting the change in λ_f. Besides the interference between SPPs and directly transmitted light (type I), which is the mechanism that creates fringes surrounding isolated holes,[22] the interference between SPPs launched from neighboring holes (type II) can also contribute to the formation of fringes in the near-field for hole arrays.

Figure 2 depicts the one-dimensional (1D) in-plane electric field of SPPs between adjacent holes and the directly
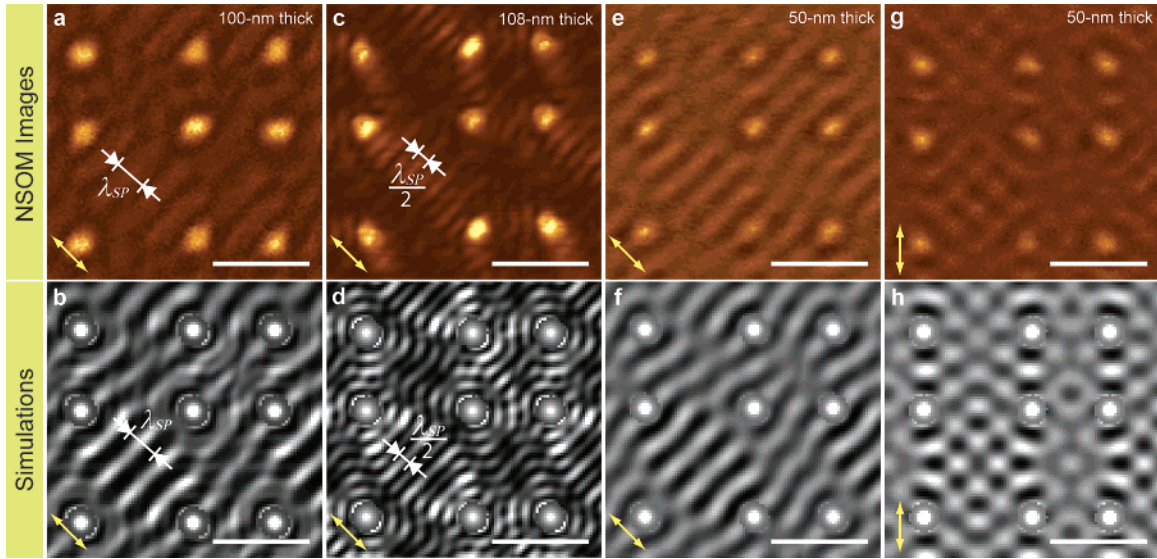
Figure 3. Experimental and simulated near-field images of nanohole arrays in gold films. (a−f) Near-field images of hole arrays with different film thickness and calculated images with different A_l/A_{SP} ratios. (g and h) Near-field and calculated images of hole arrays illuminated with light with a different polarization. Yellow arrows indicate the polarization direction of the incident light. All scale bars are 2 μm.

transmitted light under incident excitation polarized along the x-direction. The equations are

$$E_{SP1}(x) = A_{SP}e^{-x/\delta_{SP}}\cos(k_{SP}x) \qquad (1)$$

$$E_{SP2}(x) = A_{SP}e^{-(a_0-x)/\delta_{SP}}\cos(k_{SP}(a_0-x)) \qquad (2)$$

$$E_l(x) = A_l \qquad (3)$$

where A_{SP} and A_l are the amplitudes of the SPPs and the directly transmitted light at the top surface and k_{SP} is the in-plane SPP wavevector. Because $a_0 \sim 2\ \mu$m $\ll \delta_{SP}$, the decay factors $e^{-x/\delta_{SP}}$ and $e^{-(a_0-x)/\delta_{SP}}$ do not change significantly from $x = 0$ to $x = a_0$, and they can be neglected to simplify the expression. The total electric field is then reduced to

$$E_{tot}(x) = E_{SP1}(x) + E_{SP2}(x) + E_l(x) = \\ A_l + 2A_{SP}\cos(k_{SP}a_0/2)\cos(k_{SP}(2x-a_0)/2) \quad (4)$$

and the total intensity between the holes is

$$I_{tot}(x) = |E_{tot}(x)|^2 = A_l^2 + \\ 4A_lA_{SP}\cos(k_{SP}a_0/2)\cos(k_{SP}(2x-a_0)/2) + \\ A_{SP}^2\cos^2(k_{SP}a_0/2)\cos^2(k_{SP}(2x-a_0)/2) \quad (5)$$

The second term of I_{tot} (I_2) represents the interference between SPPs and directly transmitted light. The third term of I_{tot} (I_3) represents the interference between SPPs from neighboring holes. If the A_l/A_{SP} ratio is large, I_2 tends to dominate I_{tot}, and $\lambda_f = \lambda_{SP}$ (Figure 2b); if the A_l/A_{SP} ratio is small, I_3 tends to dominate I_{tot}, and $\lambda_f = \lambda_{SP}/2$ (Figure 2c). This straightforward derivation shows that two types of interference can affect the overall distribution of the near-field optical intensity and that λ_f is primarily determined by the A_l/A_{SP} ratio.

We carefully investigated a series of gold nanohole arrays with increasing film thickness ($t = 50, 75, 100, 108, 125, 150,$ and 180 nm) to test different scenarios for the two types of interference. We found that hole array films with $t < 100$ nm exhibited $\lambda_f = \lambda_{SP}$, while films with $t > 108$ nm exhibited $\lambda_f = \lambda_{SP}/2$ (Figure 3 and Supplementary Figure 1). In addition, we expanded the 1D model and simulated the two-dimensional (2D) near-field distribution with $\delta_{SP} = 10\ \mu$m, $|\vec{k}_{SP}| = 2\pi/\lambda_{SP} = 0.0104$ nm^{-1}, and the appropriate polarization angle. Parts b and d of Figure 3 depict 2D simulations for large and small A_l/A_{SP} ratios, which are in excellent agreement with NSOM images of nanohole arrays in 100 nm thick films (large A_l/A_{SP} ratio) and in 108 nm thick films (small A_l/A_{SP} ratio) (parts a and c of Figure 3). The correspondence between the experimental and theoretical images indicates that thinner films exhibit larger A_l/A_{SP} ratios; that is, the thinner the film, the greater the amplitude is of the directly transmitted light relative to the SPPs on the top surface. Depending on the competition between these two types of interference, λ_f can be either λ_{SP} or $\lambda_{SP}/2$.

To examine our model and test for SPPs further in these nanohole arrays, we changed the polarization direction of the incident light and imaged 50 nm thick gold films. Parts e−h of Figure 3 show that NSOM images and calculated patterns were also in perfect agreement. Compared to more sophisticated numerical simulations,[23] our theoretical model not only reproduces the near-field optical images but also provides an intuitive mechanism to describe how SPPs launched from nanoholes can interfere with each other. Because SPPs are only supported at the metal−dielectric interface, nonmetallic nanohole arrays should not exhibit similar fringes. NSOM measurements on a 90-nm silicon film with $a_0 \sim 2\ \mu$m did not show any features (Supplemental Figure 2), which indicates that the near-field optical fringes depend critically on the material properties and not only on geometry. This materials-dependence indicates that compos-
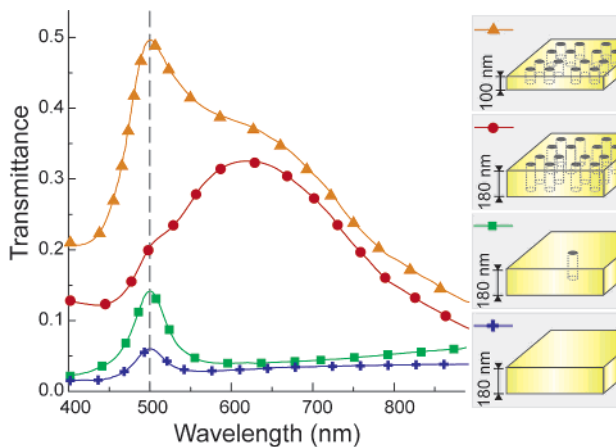
Figure 4. Transmittance of gold films, isolated holes, and nanohole arrays. Solid films (+) and single holes (■) in 180 nm thick films exhibit only an intraband transition peak at 500 nm. 250-nm hole arrays ($a_0 \sim 2\ \mu$m) in 180-nm films (●) and 100-nm films (▲) exhibit a SPP band centered around 615 nm.

ite diffracted evanescent waves[13] do not play a significant role in our system. Our combined near-field experimental and theoretical results provide direct evidence for the presence of SPPs on metallic nanohole arrays.

We have quantified how much the SPPs contribute to the optical transmission by performing far-field spectroscopic measurements of isolated holes and nanoholes in arrays (Figure 4). Zero-order transmission spectra were acquired using a 100-W halogen white light source with an optical microscope (TE−2000, Nikon) connected to a Czerny-Turner spectrometer (Triax 552, Horiba Jobin Yvon). The transmittance (defined in Supporting Information) of all gold films showed a distinct peak around 500 nm, which represents the intraband transition and is an inherent property of the gold material.[24,25] Besides this peak, isolated 250-nm holes with $t = 180$ nm did not exhibit any other features (Figure 4, ■) within the wavelength range of our measurement (400−900 nm).[26] In contrast, nanohole arrays with the same film thickness or less than the isolated hole displayed a broad band centered around 615 nm (Figure 4, ● ▲). Interestingly, the ratio of the intensity between the 500-nm peak and the 615-nm band decreased with increasing film thickness. A similar trend was also observed in the near-field results, where the A_I/A_{SP} ratio decreased with increasing film thickness. Therefore, since the amplitude of the intraband transition peak can be considered as a measure of the directly transmitted light,[27] the combined far-field and near-field results suggest strongly that the 615-nm band can be attributed to the presence of SPPs due to interactions between the holes.

The far-field spectra demonstrate, moreover, that coupling between holes is critical for enhanced transmission from SPPs. Noticeably, the 615-nm SPP band is not present in the spectrum of the isolated hole even though SPPs were observed in the near-field images. For nanoholes in an array, SPPs launched from one hole can be coupled back to free space light by scattering from adjacent holes, and hence the optical transmission can be enhanced by SPPs. In the case of isolated holes or hole arrays with $a_0 \gg \delta_{SP}$, the SPPs

launched from one hole are mostly dissipated before they can reach the adjacent holes and thus do not contribute to the light transmission around 615 nm. In our system, the transmittance of 250-nm gold hole arrays in 180-nm films is enhanced up to 8.2 times at 615 nm (comparing ● to ■ in Figure 4) because of contributions from SPPs. Thicker films are expected to exhibit even greater enhancements because the decay of light through the gold film is greater than that of the SPPs through the nanoholes.

In conclusion, we have demonstrated direct evidence for the role of SPPs in the enhanced optical transmission of light through arrays of metallic nanoscale holes. Near-field images directly confirmed the presence of SPPs; the simple interference model provided an intuitive explanation of two types of fringe wavelengths observed in NSOM images, and far-field spectra revealed a SPP band that contributed to the enhanced transmission. Silicon nanohole arrays did not exhibit any features in the near-field, which further demonstrates that metallic materials are necessary for enhanced light transmission through nanohole arrays.

Supporting Information Available: Calculation of the Au surface plasmon polariton wavelength, definition of transmittance, line scans of NSOM images, and near-field and far-field results from Si nanohole arrays. This material is available free of charge via the Internet at http://pubs.acs.org.

References

(1) Ebbesen, T. W.; Lezec, H. J.; Ghaemi, H. F.; Thio, T.; Wolff, P. A. *Nature* **1998**, *391*, 667.
(2) Pendry, J. B.; Martín-Moreno, L.; Garcia-Vidal, F. J. *Science* **2004**, *305*, 847.
(3) Barnes, W. L.; Dereux, A.; Ebbesen, T. W. *Nature* **2003**, *424*, 824.
(4) Fang, N.; Lee, H.; Sun, C.; Zhang, X. *Science* **2005**, *308*, 534.
(5) Bozhevolnyi, S. I.; Volkov, V. S.; Devaux, E.; Laluet, J.-Y.; Ebbesen, T. W. *Nature* **2006**, *440*, 508.
(6) Andrew, P.; Barnes, W. L. *Science* **2004**, *306*, 1002.
(7) Brockman, J. M.; Nelson, B. P.; Corn, R. M. *Annu. Rev. Phys. Chem.* **2000**, *51*, 41.
(8) Schuster, S. C.; Swanson, R. V.; Alex, L. A.; Bourret, R. B.; Simon, M. I. *Nature* **1993**, *365*, 343.
(9) Hayer-Hartl, M. K.; Martin, J.; Hartl, F. U. *Science* **1995**, *269*, 836.
(10) Bethe, H. A. *Phys. Rev.* **1944**, *66*, 163.
(11) Martín-Moreno, L.; Garcia-Vidal, F. J.; Lezec, H. J.; Pellerin, K. M.; Thio, T.; Pendry, J. B.; Ebbesen, T. W. *Phys. Rev. Lett.* **2001**, *86*, 1114.
(12) Cao, C.; Lalanne, P. *Phys. Rev. Lett.* **2002**, *88*, 057403.
(13) Lezec, H. J.; Thio, T. *Opt. Lett.* **2004**, *12*, 3629.
(14) Sarrazin, M.; Vigneron, J. *Phys. Rev. B* **2005**, *71*, 075404.
(15) Raether, H. *Surface Plasmons on Smooth and Rough Surfaces and on Gratings*; Springer: Berlin, 1988.

(16) Kwak, E.-S.; Henzie, J.; Chang, S.-H.; Gray, S. K.; Schatz, G. C.; Odom, T. W. *Nano Lett.* **2005**, *5*, 1963.

(17) Krishnan, A.; Thio, T.; Kim, T. J.; Lezec, H. J.; Ebbesen, T. W.; Wolff, P. A.; Pendry, J. B.; Martín-Moreno, L.; Garcia-Vidal, F. J. *Opt. Commun.* **2001**, *200*, 1.

(18) Grupp, D. E.; Lezec, H. J.; Ebbesen, T. W.; Pellerin, K. M.; Thio, T. *Appl. Phys. Lett.* **2000**, *77*, 1569.

(19) Henzie, J.; Barton, J. E.; Stender, C. L.; Odom, T. W. *Acc. Chem. Res.* **2006**, *39*, 249.

(20) Lamprecht, B.; Krenn, J. R.; Schider, G.; Ditlbacher, H.; Salerno, M.; Felidj, N. L. A.; Aussenegg, F. R. *Appl. Phys. Lett.* **2001**, *79*, 51.

(21) Popov, E.; Bonod, N.; Neviere, M.; Rigneault, H.; Lenne, P. F.; Chaumet, P. *Appl. Opt.* **2005**, *44*, 2332.

(22) Yin, L.; Vlasko-Vlasov, V. K.; Rydh, A.; Pearson, J.; Welp, U.; Chang, S.-H.; Gray, S. K.; Schatz, G. C.; Brown, D. B.; Kimball, C. W. *Appl. Phys. Lett.* **2004**, *85*, 467.

(23) Chang, S.; Gray, S. K.; Schatz, G. C. *Opt. Express* **2005**, *13*, 3150.

(24) Bohren, C. F.; Huffman, D. R. *Absorption and Scattering of Light by Small Particles*; John Wiley & Sons: New York, 1983.

(25) Shuford, K. L.; Ratner, M. A.; Gray, S. K.; Schatz, G. C. *Appl. Phys. B* **2006**, *84*, 11.

(26) Prikulis, J.; Hanarp, P.; Olofsson, L.; Sutherland, D.; Käll, M. *Nano Lett.* **2004**, *4*, 1004.

(27) Palik, E. D. *Handbook of optical constants of solids*; Academic Press: London, 1985.

NL061670R